



# NONTHERMAL X-RAY SPECTRA FROM THE JIPPT-IIU TOKAMAK

S. Morita

► To cite this version:

S. Morita. NONTHERMAL X-RAY SPECTRA FROM THE JIPPT-IIU TOKAMAK. Journal de Physique Colloques, 1988, 49 (C1), pp.C1-211-C1-214. 10.1051/jphyscol:1988141 . jpa-00227461

**HAL Id: jpa-00227461**

**<https://hal.science/jpa-00227461>**

Submitted on 4 Feb 2008

**HAL** is a multi-disciplinary open access archive for the deposit and dissemination of scientific research documents, whether they are published or not. The documents may come from teaching and research institutions in France or abroad, or from public or private research centers.

L'archive ouverte pluridisciplinaire **HAL**, est destinée au dépôt et à la diffusion de documents scientifiques de niveau recherche, publiés ou non, émanant des établissements d'enseignement et de recherche français ou étrangers, des laboratoires publics ou privés.

# NONTHERMAL X-RAY SPECTRA FROM THE JIPPT-IIU TOKAMAK

S. MORITA

*Institute of Plasma Physics, Nagoya University, Nagoya 464, Japan*

Titanium full K $\alpha$  spectra have been measured using a wide-band crystal spectrometer in lower-hybrid current drive experiments and increase in the total K $\alpha$  counts has been observed at electron densities below  $7 \times 10^{12} \text{ cm}^{-3}$ . Highly resolved titanium He-like spectra have been also measured using a high-resolution crystal spectrometer to obtain electron temperature with intensity ratio of  $I_s/I_w$  and ion temperature with w line broadening. The results show that the intensity ratio has remarkably high values and the narrowing of the w line is occurred at ohmic phase. The production of suprathermal electrons in JIPPT-IIU is described with nonthermal x-ray spectra.

## I. Full titanium K $\alpha$ emissions from LHCD plasma

The K $\alpha$  x-ray line is emitted through three processes of direct inner-shell ionization, (inner-shell) excitation and dielectronic recombination, in addition to radiative recombination. The three processes are competitive in the region of  $T_e < 1 \text{ keV}$  and the Ti K $\alpha$  emission rates from each ionic species are of the same order of magnitude (order of  $10^{-15} \text{ cm}^3 \text{ s}^{-1}$  at  $0.6 \text{ keV}$ , around  $10^{-14} \text{ cm}^3 \text{ s}^{-1}$  at  $1 \text{ keV}$ ). The intensity distributions of the full K $\alpha$  lines usually reflect the charge state distributions of the impurity ions in the plasma center, when the plasma is under the thermalized condition like normal ohmic plasmas.<sup>1)</sup>

On the other hand, in the region of  $T_e > 10 \text{ keV}$  the inner-shell ionization is a dominant process for the Ti ions and the rate drastically increases. At that time it becomes comparable with the total K $\alpha$  emission rate ( $1.5 \times 10^{-12} \text{ cm}^3 \text{ s}^{-1}$  at  $10 \text{ keV}$ ) and it is roughly constant in the region of  $10 \text{ keV}$ – $1 \text{ MeV}$ .

This indicates that a small amount of the suprathermal electrons affect the line intensities.

Typical lower-hybrid current drive (LHCD) experiments are carried out with the RF power of  $P_{\text{RF}} = 50$ – $150 \text{ kW}$  and the pulse length of about  $100 \text{ ms}$ .<sup>2)</sup> The spectra were obtained using a wide-band Johann type crystal spectrometer.<sup>3)</sup> The crystal used is Ge(220) with a bent radius of  $1 \text{ m}$ . The detector is a position-sensitive proportional counter with a spatial resolution less than  $200 \mu\text{m}$ . The system offers a spectral band width of  $0.2 \lambda$  at  $2.6 \lambda$  and a spectral resolving power of  $\lambda/\Delta\lambda \sim 300$ .

Figure 1 shows typical examples of the K $\alpha$  spectra from the LHCD plasma. The upper spectra are obtained from ohmic plasma before LHCD. The spectra can not be observed at electron temperature less than  $0.6 \text{ keV}$  as shown in Fig.1(c1). On the contrary the lower spectra from the LHCD plasma are observed with enough intensities. In addition the K $\alpha$  lines from partially M-shell-ionized ions<sup>4,5)</sup> indicated by

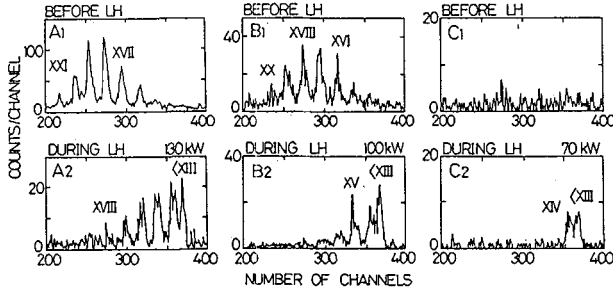


Fig.1 Ti K $\alpha$  thermal and nonthermal emissions. Upper traces show thermal emissions before LH and lower traces show nonthermal emissions during LH.

- (a1)  $n_e = 6.5 \times 10^{12} \text{ cm}^{-3}$ ,  $T_e = 0.95 \text{ keV}$   
 (a2)  $n_e = 3.0 \times 10^{12} \text{ cm}^{-3}$ ,  $T_e = 0.55 \text{ keV}$   
 (b1)  $n_e = 6.0 \times 10^{12} \text{ cm}^{-3}$ ,  $T_e = 0.85 \text{ keV}$   
 (b2)  $n_e = 2.5 \times 10^{12} \text{ cm}^{-3}$ ,  $T_e = 0.50 \text{ keV}$   
 (c1)  $n_e = 3.5 \times 10^{12} \text{ cm}^{-3}$ ,  $T_e = 0.55 \text{ keV}$   
 (c2)  $n_e = 2.5 \times 10^{12} \text{ cm}^{-3}$ ,  $T_e < 0.40 \text{ keV}$

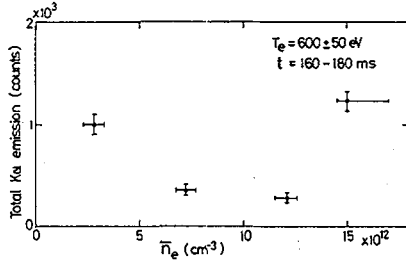


Fig.2 Electron density dependence of total Ti K $\alpha$  emissions.

<XIII> are dominant. These features are typical of nonthermal plasmas with high energy electron component. Hence, the total counts of the K $\alpha$  spectra are sensitive to efficiencies of the LHCD as shown in Fig.2. In this case the LHCD is growing at electron densities below  $7 \times 10^{12} \text{ cm}^{-3}$ .

## II. Intensity ratio of $I_s/I_w$

Intensity ratio  $I_s/I_w$  of  $n \approx 3$  Li-like dielectronic satellites to He-like resonance line is measured to obtain electron temperature as shown in Fig.3. In this calculation we use a following simple equation:

$$T_e (\text{keV}) = C_0 + C_1(R-2.5) + C_2(R-2.5)^2 + C_3(R-2.5)^3$$

where  $C_0 = 1.3224$ ,

$$C_1 = 3.8285 \times 10^{-1},$$

$$C_2 = -1.3394 \times 10^{-2},$$

$$C_3 = 5.2031 \times 10^{-3},$$

$$R = I_2/I_1$$

$$I_1 = I_w + I_{s1}, \quad I_2 = I_{s2}, \quad I_s = I_{s1} + I_{s2},$$

$$(I_1: 2.6075-2.6107 \text{ \AA} \quad I_2: 2.6107-2.6153 \text{ \AA}).$$

However, the intensity ratio does not reflect the electron temperature, when suprathermal electrons exist in the plasma. Because excitation rate by electron impact of the He-like resonance line becomes drastically large in the energy range of more than 10 keV. A typical example is shown in Fig.4. The suprathermal electrons with energies of more than 30 keV are produced during fast wave injection<sup>6)</sup> and the He-like resonance line is rapidly enhanced whereas the bulk electron temperature is not changed. In that case we can determine the quantity of the suprathermal electrons using the additional enhancement of the resonance line. The equation for the calculation is given by Bartiromo et al.<sup>7)</sup> and we modified it as follows;

$$n_T = 397.6(1/R_e - 1/R_t)(0.0136/T_e)^{3/2} \exp(-4.141/T_e)$$

$$R_t = 2.47 \times 10^{-9}(0.0136/T_e)^{3/2} \exp(-4.141/T_e) / \langle \sigma v \rangle$$

$$R_e = I_2/I_w = 1/(I_1/I_2 - 0.452),$$

where  $\langle \sigma v \rangle$  is excitation rate of the He-like resonance line. From this equation the increment in the fractional density  $n_s$  of suprathermal electrons by the rf is estimated to be about 0.8% ( $=n_T$ ) of the bulk electron density.

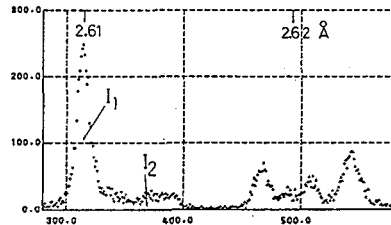


Fig.3 High-resolution TiXXI He-like spectrum.

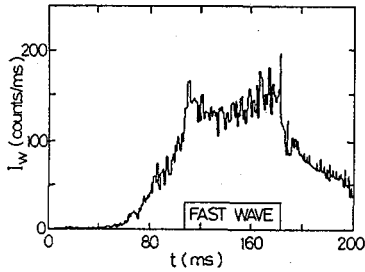


Fig.4 Time behaviour of TiXXI He-like resonance line  $I_w$  in fast wave injection experiment.

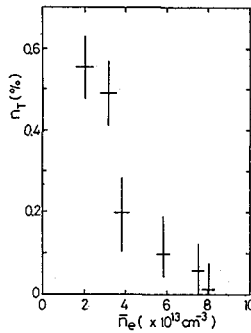


Fig.5 Fractional amount  $n_T (=n_s/n_e)$  of the suprathermal electrons as a function of electron density.

The similar method is adopted also to the ohmic discharges. The results are shown in Fig.5. The fractional amount of the suprathermal (or runaway) electrons becomes less than 0.01% at the line-averaged density of  $8 \times 10^{13} \text{ cm}^{-3}$ . Error bars mainly depend on evaluation of the continuum background level, since the intensity of the dielectronic satellites is relatively weak.

It should be noticed that these values are some standard to describe the development of the runaway electrons in tokamak. Because the x-ray spectra obtained are an integration of the line of sight along the radial direction. The radial distribution of the runaway electrons does not always correspond to that of the Ti He-like ions, as described in section III.

### III. Narrowing of He-like resonance line

The ion temperature has been measured systematically using Doppler broadening of the He-like resonance line with high-resolution crystal spectrometer. The spectral resolution  $\lambda/\Delta\lambda$  is roughly more than  $2 \times 10^4$  and the lowest ion temperature which can be measured is  $\sim 300 \text{ eV}$ . Raw data from it are shown in Fig.6. The profiles are fitted with Voigt function. ICRF wave for additional heating is injected for a period of 130-190ms. Broadened spectral features are clearly observed during ICRF heating and we notice that the line is shifted toward the toroidal direction. The toroidal rotation is related with plasma potential.<sup>8)</sup>

The ion temperature obtained is shown in Fig.7. It is in good agreement with one from Fast Neutral Analyzer in the ICRF heating phase producing high temperature and high density plasma ( $T_e = 2 \text{ keV}$ ,  $n_e = 1 \times 10^{14}$ ). In the ohmic phase, however, the ion temperature from the crystal spectrometer always yields lower values compared with FNA.

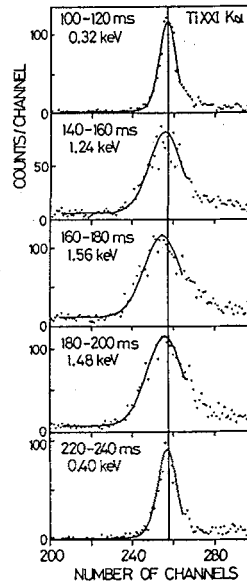


Fig.6 Time-resolved TiXXI w line profiles.

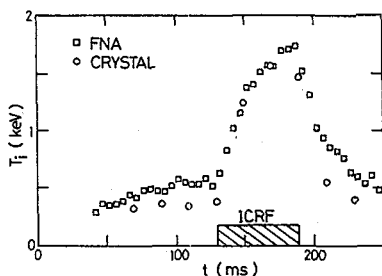
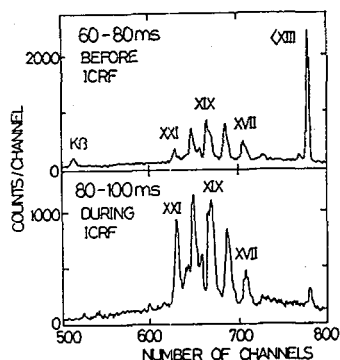


Fig.7 Time behaviours of ion temperature.

Fig.8 Runaway-dominant Ti K $\alpha$  spectra.

Narrowing of the He-like resonance line is occurred. It is difficult to treat the difference accurately, since the difference is considerably small.

The He-like resonance line intensity increases with development of the runaway electrons, and a large amount of the runaway electrons is frequently observed at the outer region of the plasma where the ion temperature is relatively low. An extreme example of it is shown in Fig.8. In this case the amount is reduced during ICRF heating because of the increase in the electron density. The narrowing is caused by the runaway electrons which are developed at the cooler region of the plasma.

#### Acknowledgement

The author acknowledges Prof.J.Fujita and members of JIPPT-IIU group for their helpful discussions and encouragement.

#### References

- 1) K.W.Hill, S.von Goeler, M.Bitter et al., Phys.Rev.A **19**(1979)1770.
- 2) K.Ohkubo and K.Matsumoto, Jpn.J.Appl.Phys. **26**(1987)142.
- 3) S.Morita and J.Fujita, Nucl.Instrum.Methods **139**(1985)713.
- 4) S.Morita, K.Kadota, T.Kagawa and J.Fujita, Phys.Lett. **94A**(1983)147.
- 5) S.Morita and J.Fujita, Phys.Rev.A **31**(1985)3299.
- 6) K.Toi et al., IPPJ-828(1987).
- 7) R.Bartirromo et al., Phys.Rev.A **32**(1985)531.
- 8) S.Morita et al., Proc.14th Europ.Conf.on Controlled Fusion and Plasma Physics, Madrid (1987).